Article

A DFT Study of the Thermal, Orbital Symmetry Forbidden, Cyclophanediene to Dihydropyrene Electrocyclic Reaction. Predictions to Improve the Dimethyldihydropyrene Photoswitches

Richard Vaughan Williams, W. Daniel Edwards, Reginald H. Mitchell, and Stephen G. Robinson

J. Am. Chem. Soc., **2005**, 127 (46), 16207-16214• DOI: 10.1021/ja054553r • Publication Date (Web): 28 October 2005

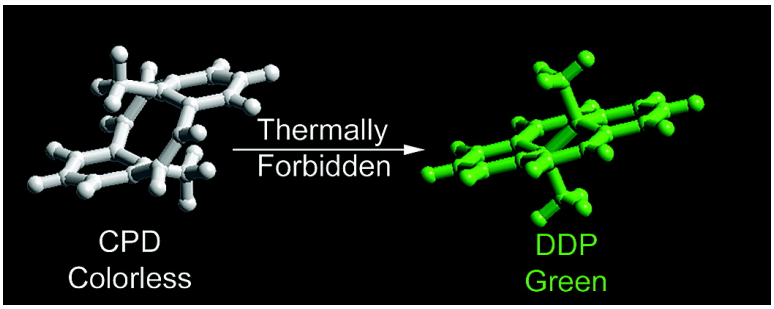

More About This Article

Additional resources and features associated with this article are available within the HTML version:

- Supporting Information
- Links to the 8 articles that cite this article, as of the time of this article download
- Access to high resolution figures
- Links to articles and content related to this article
- Copyright permission to reproduce figures and/or text from this article

View the Full Text HTML

J|A|C|S
ARTICLES
Published on Web 10/28/2005

A DFT Study of the Thermal, Orbital Symmetry Forbidden, Cyclophanediene to Dihydropyrene Electrocyclic Reaction. Predictions to Improve the Dimethyldihydropyrene Photoswitches

Richard Vaughan Williams,*,† W. Daniel Edwards,† Reginald H. Mitchell,*,‡ and Stephen G. Robinson‡

Contribution from the Department of Chemistry, University of Idaho, PO Box 442343, Moscow, Idaho 83844-2343, and Department of Chemistry, University of Victoria, PO Box 3065, Victoria, BC, Canada V8W 3V6

Received July 8, 2005; E-mail: williams@uidaho.edu

Abstract: The orbital symmetry forbidden thermal electrocyclic equilibria between a series of cyclophanedienes and dimethyldihydropyrenes (CPDs⇄DDPs) were studied using density functional theory (DFT). These reactions are important not only because of their fundamental interest but also in how they restrict the potential utility of the DDP photoswitches by limiting the thermal lifetime of the CPDs. The transition states (TSs) for these reactions could not be modeled using restricted DFT (RB3LYP) but were located using unrestricted DFT (UB3LYP). Each TS possesses significant biradical character as indicated by their spin contaminated wave functions, $\langle S^2 \rangle \neq 0$. Specific substitution by nitrile or trifluoromethyl group(s) is predicted to strongly affect the magnitude of the activation barriers for these reactions. In particular, replacing the internal methyl groups of the CPDs/DDPs with nitrile groups is predicted to have the maximum effect and to raise the activation barriers and lifetimes of the CPDs considerably.

Introduction

Dimethyldihydropyrenes (DDPs) are not only key molecules in our quest to understand aromaticity,[1] but they are also proving to be extremely interesting molecular switches.[2a] They belong to the important diarylethene class of photochromes,[2b] and while they lack the excellent thermal bistability shown by Irie's[2c] dithienylethenes, they have the advantage that the photostationary equilibrium lies well to one side or the other, that is, they can completely open and close rather than form mixtures containing substantial amounts of each isomer.[2d] As well, our DDPs can be synthesized to give multiple π-state switches[2d] and be linked together and remain fully photochromic.[2e]

Although thermochromic compounds can be useful for certain applications, a limitation of DDPs as molecular switches is the restricted lifetime of the colorless cyclophanedienes (CPDs), which undergo facile thermal return to their corresponding colored DDPs. These thermal return electrocyclization reactions are forbidden by the rules of conservation of orbital symmetry.[3] Orbital symmetry, or Woodward−Hoffmann (W−H),[4] forbidden reactions are a continuing source of fascination and area of study for both experimentalists and theorists.[5,6] In general and where possible, the W−H allowed path is followed in pericyclic reactions. However, where constraints, such as the geometrically enforced *con*rotatory closure of the CPD to the DDP, render the W−H forbidden path the only one accessible, then the reaction may proceed by this *forbidden* path. The salient characteristic of a W−H forbidden reaction is the correlation of occupied reactant and product orbitals with virtual orbitals of the appropriate symmetry (an occupied reactant orbital correlates with an unoccupied product orbital and vice versa). This correlation leads to an orbital crossing which is normally manifested in an avoided crossing (of states of the same symmetry) in that reaction's state correlation diagram (Figure 1). The avoided crossing results in an appreciable activation barrier for reaction and is the origin of the forbiddenness. Because of the orbital crossing, a necessary consequence of the symmetry mandated correlation of occupied orbitals with virtual orbitals, W−H forbidden reactions can only be adequately modeled by calculations incorporating electron correlation.

Schmidt, in his extended-Hückel study of the parent CPD (**1**) → DDP (**1a**) thermal ring closure, pointed out the necessity of including electron correlation in these calculations.[3] Subse-

† University of Idaho.
‡ University of Victoria.

(1) Mitchell, R. H. *Chem. Rev.* **2001**, *101*, 1301; *Adv. Theor. Interesting Mol.* **1989**, *1*, 135.
(2) (a) Mitchell, R. H. *Eur. J. Org. Chem.* **1999**, 2695. (b) Irie, M. (Guest Editor) *Chem. Rev.* **2000**, *100*, 1683. (c) Irie, M. *Chem. Rev.* **2000**, *100*, 1685. (d) Mitchell, R. H.; Ward, T. R.; Chen, Y.; Wang, Y.; Weerawarna, S. A.; Dibble, P. W.; Marsella, M. J.; Almutairi, A.; Wang, Z. Q. *J. Am. Chem. Soc.* **2003**, *125*, 2974. (e) Mitchell, R. H.; Bandyopadhyay, S. *Org. Lett.* **2004**, *6*, 1729.
(3) Schmidt, W. *Helv. Chim. Acta* **1971**, *54*, 862.
(4) Woodward, R. B.; Hoffmann, R. *The Conservation of Orbital Symmetry*; Verlag Chemie: Weinheim, Germany, 1970.
(5) Reviews: (a) Baldwin, J. E.; Andrist, A. H.; Pinschmidt, R. K., Jr. *Acc. Chem. Res.* **1972**, *5*, 402. (b) Berson, J. A. *Acc. Chem. Res.* **1972**, *5*, 406. (c) Baldwin, J. E. *Org. Chem.* **1977**, *35*, 273.
(6) For some recent studies, see the following and references therein: (a) Leach, A. G.; Catak, S.; Houk, K. N. *Chem.—Eur. J.* **2002**, *8*, 1290. (b) Baldwin, J. E.; Burrell, R. C. *J. Am. Chem. Soc.* **2003**, *125*, 15869.

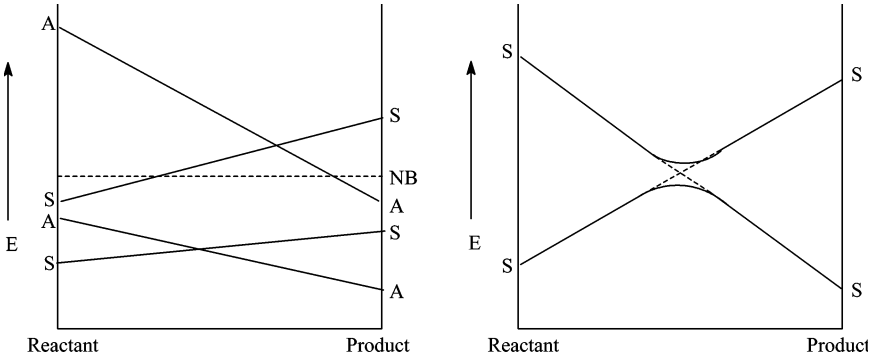

Figure 1. Schematic representations of a partial orbital correlation diagram (left) and a partial state correlation diagram (right) for a hypothetical W−H forbidden reaction. The dashed line (NB) represents the nonbonding level, and A and S correspond with arbitrarily assigned orbital or state symmetry (anti-symmetric and symmetric, respectively).

quently, Baldwin, in two nice review articles, forcefully made the case that for meaningful calculations on W−H forbidden reactions inclusion of electron correlation is essential.[5a,c] Not surprisingly, without electron correlation, it has sometimes proved impossible to even locate a transition structure for a W−H forbidden reaction.[7] As expected, inclusion of electron correlation, as it must be to represent these forbidden systems with their orbital crossing, results in a lowering of the energy of the transition state and often an accessible activation barrier for these *forbidden* reactions.

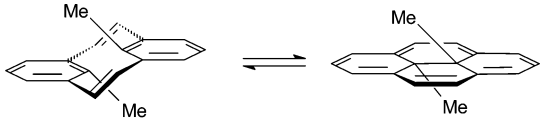

1 **1a**

Substituent effects on the rate of the CPD → DDP thermal reaction are small (Arrhenius activation energies vary between $E_a \sim 20-24$ kcal/mol for a wide range of substituted and annelated CPDs[2]) and appear not to follow any particular trend. It is desirable to be able to exert predictable control over the rate of these thermal return reactions and to design CPDs with extended lifetimes. To this end, we undertook the present study with the goal of elucidating the mechanism of the thermal return reaction. A knowledge of this mechanism could lead to strategies to control the lifetime of the CPDs.

Results and Discussion

Computational Methods. Density functional theory (DFT) using the B3LYP/6-31G* method is very successful in modeling DDPs and a variety of other aromatic systems.[8] B3LYP/6-31G* is also known to accurately model pericyclic processes and their experimental activation barriers.[6a,9] We used this method, as instituted in Gaussian 98,[10] to calculate the structures and energies of 21 pairs of CPDs and DDPs along with their corresponding transition states (TSs). Analytical energy second derivatives were calculated at all optimized structures to confirm that these are minima (zero imaginary frequencies) or transition states (one imaginary frequency).

Table 1. Energy Differences in kcal/mol (temperature, K) for **1/1*/1a**, **1b/1b*/1c**, **2/2*/2a**, and **2b/2b*/2c**

	ΔH	ΔH_{expt}	ΔG (298)	ΔG_{expt}	E_A
1−**1a**	23.184		21.322	2.3 (298)[a]	
1*−**1**	20.301	22.4[a]	20.900		23.0[a], 22.2[b]
1*−**1a**	43.485		42.223		
1b−**1c**	22.250		20.429		
1b*−**1b**	20.552	23.3[c]	21.140		24.0[c], 21.8[b]
1b*−**1c**	42.802		41.569		
2−**2a**	−8.771		−8.987		
2*−**2**	24.435		25.474		
2*−**2a**	15.665		16.487		
2b*−**2c**		20[c]			20[c]

[a] Reference 13. [b] Murakam, S.; Tsutsui, T.; Saito, S.; Yamato, T.; Tashiro, M. *Nippon Kagukukai Shi* **1988**, 221−229. [c] Reference 2d.

The Parent CPD 1 and DDP 1a. We have previously reported the results of our B3LYP/6-31G* calculations on DDP (**1a**).[8b] The minimum energy structure of CPD **1**, like **1a** is of C_{2h} symmetry, was easily located and, as expected, proved to be thermodynamically less stable than **1a** ($\Delta H = 23.184$ kcal/mol, Table 1). The magnitude of the B3LYP/6-31G* enthalpy difference between **1** and **1a** is much larger than was reported previously (~3.4 kcal/mol). This discrepancy is not unexpected as the previous extended-Hûckel[3] and semiempirical (AM1)[11] calculations do not include electron correlation which will have a greater effect on the fully conjugated (14-π) **1a** than on the two isolated phenyl rings (6-π) of **1**. We have shown that incorporation of electron correlation is essential in modeling DDP **1a**.[12] Without electron correlation, AM1 yields a bond alternating structure for **1a** about 10 kcal/mol lower in energy than the correct bond equalized structure. Inclusion of correlation in the AM1 calculation through a simple 4 × 4 configuration interaction (CI4) correctly gives the bond equalized structure as the low energy form. The correlated (AM1 CI4) heat of formation (ΔH_f) for the bond equalized structure is about 17 kcal/mol less than the corresponding AM1/SCF ΔH_f. Similarly, single-point Hartree−Fock (HF) 6-31G* calculations on the

(7) Spellmeyer, D. C.; Houk, K. N.; Rondan, N. G.; Miller, R. D.; Franz, L.; Fickes, G. N. *J. Am. Chem. Soc.* **1989**, *111*, 5356.
(8) See, for example, the following and references therein: (a) Mitchell, R. H.; Blunden, R.; Hollet, G.; Bandyopadhyay, S.; Williams, R. V.; Twamley, B. *J. Org. Chem.* **2005**, *70*, 675. (b) Williams, R. V.; Armantrout, J. R.; Twamley, B.; Mitchell, R. H.; Ward, T. R.; Bandyopadhyay, S. *J. Am. Chem. Soc*. **2002**, *124*, 13495. (c) Kimball, D. B.; Haley, M. M.; Mitchell, R. H.; Ward, T. R.; Bandyopadhyay, S.; Williams, R. V.; Armantrout, J. R. *J. Org. Chem.* **2002**, *67*, 8798. (d) Boydston, A. J.; Haley, M. M.; Williams, R. V.; Armantrout, J. R., *J. Org. Chem.* **2002**, *67*, 8812.
(9) Hrovat, D. A.; Williams, R. V.; Quast, H.; Borden, W. T. *J. Org. Chem.* **2005**, *70*, 2627.
(10) Frisch, M. J. et al. *Gaussian 98*, revision A.9; Gaussian, Inc.: Pittsburgh, PA, 1998.
(11) Mitchell, R. H.; Iyer, V. S.; Mahadevan, R.; Venugopalan, S.; Zhou, P. *J. Org. Chem.* **1996**, *61*, 5116.
(12) Williams, R. V.; Edwards, W. D.; Vij, A.; Tolbert, R. W.; Mitchell, R. H. *J. Org. Chem.* **1998**, *63*, 3125.

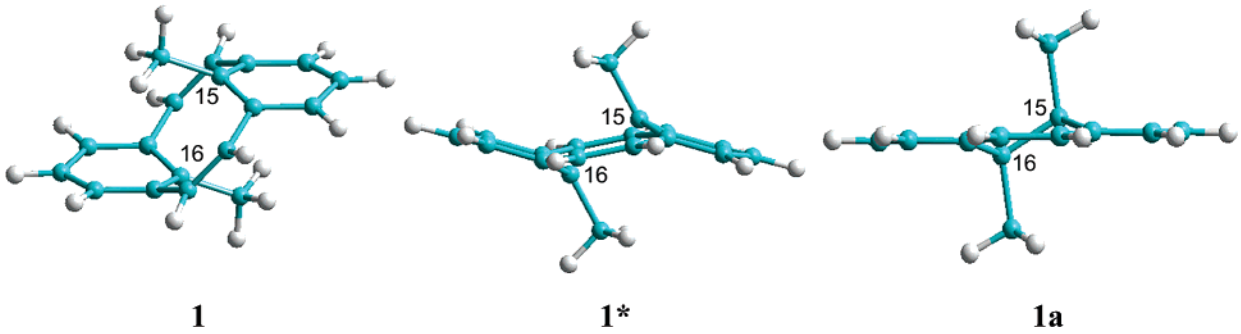

Figure 2. The optimized structures for **1**, **1***, and **1a**.

B3LYP/6-31G* optimized geometries of **1** and **1a** raise the total energy of **1a** by 14.029 kcal/mol more than the energy of **1** is raised compared with the corresponding B3LYP/6-31G* energies. At the HF/6-31G*//B3LYP/6-31G* level, **1a** is only 9.675 kcal/mol (total energy) more stable than **1**.

There is only one report of an experimental energy difference between **1** and **1a** (ΔG_{298} = 2.3 kcal/mol).[13] This value was obtained by Blattmann and Schmidt from the equilibrium constant for the high temperature thermal opening of **1a** estimated from UV/vis spectra at 70 °C. Because only very little of the CPD form is claimed to be present by the authors (about 3%), this experimental value must be viewed with caution. We studied solutions of both **1a** and **1** held at 70 °C by 300 and 500 MHz ^{1}H NMR spectroscopy. Starting with **1a**, *no peaks* corresponding to **1** could be seen in a thoroughly degassed oxygen-free benzene-d_6 solution held at 70 °C for several days. If **1a** was partially photo-opened to **1**, and then this solution was heated to 70 °C, all peaks for **1** were rapidly replaced by those of **1a**, and then the spectrum did not change further when held for several days at 70 °C. Under these circumstances, the amount of CPD present is <1%. It is therefore probable that Blattman's experimental energy difference is much too low. Unfortunately, when one component is present in very small amount, neither the NMR nor this implementation of the UV/vis method gives good ΔG values. Blattman's value for ΔG gives an equilibrium constant of 29.235 at 70 °C, and thus only 3.3% CPD would have been present, an amount very difficult to detect accurately from the change in DDP absorptions in the visible spectra.

The thermal closure of **1** to give **1a**, despite being a W−H forbidden process, is concerted.[3] Locating the transition structure **1*** for the **1**⇄**1a** reaction proved to be remarkably difficult. All attempts using restricted B3LYP (RB3LYP) theory resulted in failure. Using unrestricted B3LYP (UB3LYP), which allows

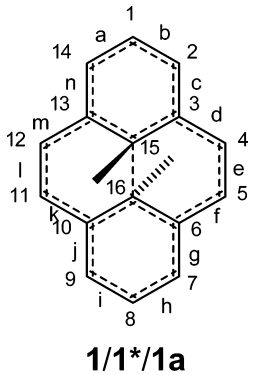

1/1*/1a

Figure 3. Numbering scheme used throughout this study.

open shell character, we were able to find **1*** by means of the quadratic synchronous transit (QST) method as implemented in Jaguar 4.0.[14] The resulting species was reoptimized to a transition state (**1***) of C_{2h} symmetry using G98, UB3LYP/6-31G*. Analytical energy second derivatives were calculated and confirmed that **1*** is a true transition structure (one imaginary frequency). Visualization of the normal mode corresponding with the imaginary frequency for this TS (and several other of the TSs found) revealed that the displacements were consistent with the CPD⇄DDP interconversion. The large spin contamination of the wave function at **1*** ($\langle S^2\rangle$ = 1.03) corresponds with an approximately 1:1 mixture of singlet ($\langle S^2\rangle$ = 0) and triplet ($\langle S^2\rangle$ = 2) states and indicates significant biradical character in **1***. This breaking of spin symmetry is probably a manifestation of a crossing of the singlet and triplet surfaces on the restricted potential energy surface, resulting in an amelioration of the forbiddenness of the CPD⇄DDP thermal electrocyclic processes.[15] The transition states for a wide variety of pericyclic reactions, especially those that are W−H forbidden, have been found to be biradical-like.[16] Mulliken population analysis (total atomic spin densities are used throughout) predicts, as expected, the highest degree of radical character at C15/C16 (0.413 unpaired electrons on each atom). The calculated enthalpy of activation for **1** to **1***, $\Delta H^{\ddagger}$ = 20.362 kcal/mol (Table 1), is in good agreement with the experimental value of $\Delta H^{\ddagger}$ = 22.4 kcal/mol.[13]

The structure of **1*** is intermediate between that of **1** and **1a** (Supporting Information Table S1). A characteristic for the whole series of CPDs, TSs, and DDPs studied herein (vide infra) is the increasing lack of planarity of the ring, C1 to C14, in going from the essentially planar DDPs to the highly stepped CPDs. In the interest of maintaining consistent atom numbering between the CPDs, TSs, and DDPs, we adopt the numbering scheme shown in Figure 3.[17] The C15−C16 distance, 2.736, 2.101, and 1.544 Å in **1**, **1***, and **1a**, respectively, is an effective indicator of this increasing nonplanarity. Although, it should be noted that in **1**, **1***, and **1a** (Figure 2) and all of the other CPDs, TSs, and DDPs, the bowsprit carbons (C15 and C16) are significantly canted away from each other and out of planarity with the rest of their "benzene" ring atoms (C1C2C3C13C14 and C6 to C10). The pseudo-dihedral angle C15C13C3C2

(13) Blattmann, H. R.; Schmidt, W. *Tetrahedron* **1970**, *26*, 5885.
(14) *Jaguar*, version 4.0; Schrödinger, Inc.: Portland, OR, 1991−2000.
(15) Özkan, I.; Kinal, A.; Balci, M. *J. Phys. Chem. A* **2004**, *108*, 507.
(16) See, for example: (a) Borden, W. T. *Mol. Phys.* **2002**, *100*, 337. (b) Kless, A.; Nendel, M.; Wilsey, S.; Houk, K. N. *J. Am. Chem. Soc.* **1999**, *121*, 4524. (c) Sakai, S.; Takane, S. *J. Phys. Chem. A* **1999**, *103*, 2878. (d) Jarzecki, A. A.; Gajewski, J.; Davidson, E. R. *J. Am. Chem. Soc.* **1999**, *121*, 6928. (e) Reference 7.
(17) For the correct IUPAC numbering see, for example: Cerfontain, H.; Koeberg-Telder, A.; Bakker, B. H.; Mitchell, R. H.; Tashiro, M. *Liebigs Ann. Recueil* **1997**, 873.

Table 2. Energies (kcal/mol), $\langle S^2 \rangle$, and Total Atomic Spin Densities for **1/1*/1a** and **2/2*/2a**

	total energy	total energy + ZPE	$\langle S^2 \rangle$	unpaired electrons C15/C16
1 (C_{2h})	−436413.3	−436235.7		
1* (C_{2h})	−436390.4	−436215.2	1.03	0.413
1a (C_{2h})	−436437.0	−436258.2		
1b (C_2)	−633771.5	−633452.2		
1b* (C_2)	−633748.4	−633431.4	1.01	0.398
1c (C_2)	−633794.2	−633473.8		
2 (C_{2h})	−629257.5	−436258.2		
2* (C_{2h})	−629231.0	−628995.6	0.76	0.228
2a (C_{2h})	−629248.7	−629011.4		

provides a measure of the extent of this canting (Supporting Information Table S1).

Di-*tert*-butyl-CPD 1b and -DDP 1c. We have shown both by B3LYP/6-31G* calculations and X-ray crystallography that the structure of the dihydropyrene nucleus is little affected by di-^{t}butyl substitution at the 1- and 8-positions (numbering of Figure 3).[8b] Similarly, the calculated structures of the di-^{t}butyl and parent CPDs and TSs are essentially equivalent (Supporting Information Table S1). The energy differences reported in Table 1 for the **1**/**1***/**1a** and **1b**/**1b***/**1c** series are very similar, and once more, the ^{t}Bu substituents appear to have little overall effect.

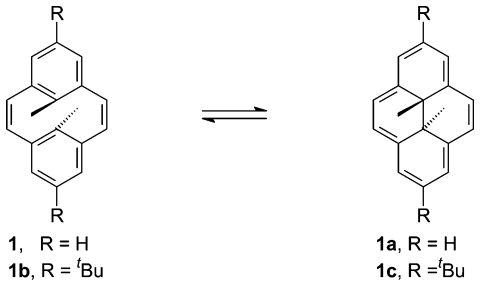

Dibenzo[e,l]-CPD 2 and -DDP 2a. While our NMR results clearly demonstrate that Blattman's free energy difference between CPD **1** and DDP **1a** is wrong, they only establish a lower limit for this difference ($\Delta G \geq 4.0$ kcal/mol). To further probe the reliability of our calculated relative energies, we investigated the dibenzo[e,l]-CPD and -DDP pair **2** and **2a**. It is known that for the di-^{t}butyl analogues of **2**/**2a**, in contrast with **1** and almost all other CPD⇄DDP equilibria, CPD **2b** is thermodynamically more stable than DDP **2c**.[18] In agreement with the experimental results for **2b**/**2c**, our calculations (Table 1) for the computationally more economical **2**/**2***/**2a** system show the CPD **2** to be lower in energy than the DDP **2a** (ΔG_{298} = 8.771 kcal/mol). The AM1 difference in ΔH_f values (18.1 kcal/mol) for **2**/**2a** correctly predicts that **2** is more stable than **2a**,[11] but overestimates the thermodynamic advantage due to the lack of electron correlation. Both the activation energy and enthalpy for the thermal reversion of **2c** to **2b** have been determined to be 20(±1) kcal/mol.[18,2d] In general, our calculated activation enthalpies ($\Delta H^{\ddagger}$) for CPDs→DDPs tend to be smaller than the experimentally determined values. This underestimation of activation enthalpy is a well recognized consequence of the use of unrestricted theory in which correlation energy is overestimated when spin contamination is high (large $\langle S^2 \rangle$).[15,19] There

(18) Mitchell, R. H.; Chen, Y. *Tetrahedron Lett*. **1996**, *37*, 5239.
(19) Staroverov, V. N.; Davidson, E. R. *J. Mol. Struct. THEOCHEM* **2001**, *573*, 81.

Table 3. Energy Differences in kcal/mol (temperature, K) for **3/3*/3a**−**7b/7b*/7**

	ΔH	ΔH_{expt}[a]	ΔG (298)	ΔG_{expt}	E_A[a]
3−**3a**	23.153		21.918		
3*−**3**	19.113		19.367		
3*−**3a**	42.266		41.285		
4−**4a**	9.502		8.196		
4*−**4**	22.614	23.8	23.732		24.6
4*−**4a**	32.117		31.928		
5−**5a**	6.812		5.899		
5*−**5**	21.664	21.4	22.441		22.1
5*−**5a**	28.476		28.340		
6−**6a**	5.553		4.722		
6*−**6**	21.045	18.4	21.995		19.1
6*−**6a**	26.598		26.7168		
7−**7a**	3.865		2.389		
7*−**7**	23.918		24.987		
7*−**7a**	27.782		27.376		
7b−**7c**	4.826		3.594		
7b*−**7b**	23.774	25.2	24.465		26.1
7b*−**7c**	28.600		28.059		

[a] Experimental values for the 1,8-di-^{t}Bu derivative from ref 2d.

is a loose correlation between the degree of spin contamination and the underestimation of the activation enthalpy with the largest deviation of 2.784 kcal/mol for **1b*** ($\langle S^2 \rangle$ = 1.01). No trend could be discerned for differences in calculated activation enthalpies between the ^{t}Bu and the unsubstituted series for the parent and furano[e]- systems (the only ones for which we examined both the ^{t}Bu and unsubstituted series) except to note that these differences are small (<1 kcal/mol). Thus, we consider our calculated activation parameters for **2a** (Table 1) to be in reasonable agreement with the experimental data for **2b**.

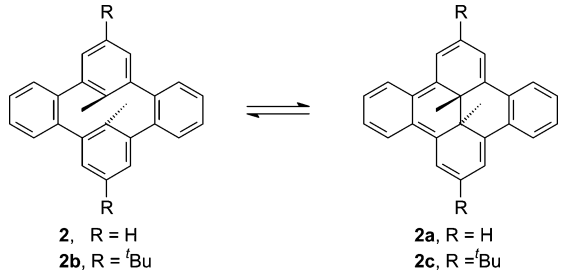

We have previously reported selected B3LYP/6-31G* structural parameters for **2a** and **2c** in our general study of the relative aromaticities of a series of annelated DDPs.[8b] The structures of **1**and **2**, **1*** and **2***, and **1a** and **2a** are quite similar (Supporting Information Table S1). The major differences between these related structures are that the annelated bonds C4−C5 (C11−C12) in **2**, **2***, and **2a** are calculated to be significantly longer than those in **1**, **1***, and **1a**, a somewhat shorter C15−C16 distance is calculated for **2*** than **1*** and the pseudo-dihedral angle (C15C13C3C2) in **2*** is markedly smaller than in **1***. The closer approach of C15 and C16 and the smaller pseudo-dihedral angle in **2*** than in **1*** is explained by the reduced biradical character in **2*** ($\langle S^2 \rangle$ = 0.76) and, from Mulliken population analysis, only 0.228 unpaired electrons on C15/C16 (Table 2).

Annelated Derivatives

The DDP form is calculated and observed (for the 1,8-di-^{t}Bu derivatives in some cases) to be lower in energy than the CPD for each of the annelated derivatives **3**−**7** (Table 3). The calculated difference in energy between the DDP and the CPD steadily decreases progressing along the series **3** to **7**. Similarly,

Table 4. Energies (kcal/mol), $\langle S^2 \rangle$, and Total Atomic Spin Densities for **3/3*/3a**−**7b/7b*/7**

	total energy	total energy + ZPE	$\langle S^2 \rangle$	unpaired electrons C15 (C16)
3 (C_1)	−532826.2	−532618.9		
3* (C_1)	−532804.6	−532599.7	0.97	0.405 (0.370)
3a (C_1)	−532850.0	−532641.6		
4 (C_2)	−532835.4	−532628.2		
4* (C_2)	−532810.6	−532605.2	0.91	0.317
4a (C_2)	−532845.5	−532637.2		
5 (C_2)	−629249.0	−629012.2		
5* (C_2)	−629224.9	−628990.3	0.85	0.285
5a (C_2)	−629256.2	−629018.6		
6 (C_2)	−725658.6	−725392.6		
6* (C_2)	−725635.3	−725371.2	0.79	0.265
6a (C_2)	−725664.6	−725397.8		
7 (C_2)	−531441.6	−531253.1		
7* (C_2)	−531415.1	−531228.8	0.88	0.292
7a (C_2)	−531445.7	−531256.4		
7b (C_2)	−728799.6	−728469.3		
7b* (C_2)	−728773.3	−728445.3	0.88	0.290
7c (C_2)	−728804.7	−728473.7		

the activation barriers for the electrocyclization of the CPD to the corresponding DDP and the degree of spin contamination in the TSs decrease down the series, and the experimental (for the 1,8-di-^{t}Bu derivatives) and calculated activation barriers are generally in good agreement. In this series, the experimental activation enthalpy is the least reliable for the 1,8-di-^{t}Bu-derivative of **6**/**6a** (estimated error ∼±1.5 kcal/mol). The spin contamination (Table 4) for **6*** ($\langle S^2 \rangle = 0.79$) is small, leading to the expectation of a closer agreement between the calculated and experimental $\Delta H^{\ddagger}$ values for **6**/**6a**. Consequently, the reported experimental $\Delta H^{\ddagger}$ is most likely low.

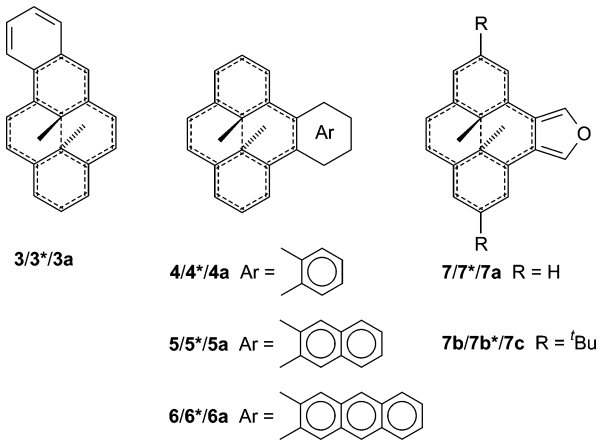

The structural trends in this series (Supporting Information Table S2) parallel those calculated and discussed for **1**−**2**. As previously reported,[8b] mono- or unsymmetrical bis-arenoannelation of DDP **1a** results in bond alternation accompanied by a reduction in the aromaticity of DDP nuclei.

Substituted Derivatives

The calculated (Table 5) differences in energy between the CPDs and DDPs in this series (**8**−**11**) are all very similar with the DDPs substantially favored over the CPDs. The calculated activation barriers and spin contamination of the TSs are also very similar across this series. Unfortunately, only one $\Delta H^{\ddagger}$ has been measured experimentally. Direct comparison of our calculated activation parameters with the experimental Arrhenius activation energies is, of course, not possible. However, the trends in experimental and calculated activation barriers are well-correlated. Acyl substitution at the 1-position results in a slight lowering of the activation barrier, whereas substitution at the 4-position is calculated to give a barrier about the same as that in the parent **1**/**1***/**1a** while the experimental activation energies (for the 1,8-di-^{t}Bu derivatives) are inconclusive as di-^{t}Bu-**10**/**10***/**10a** is somewhat lower and di-^{t}Bu-**11**/**11***/**11a** is somewhat higher than in **1**/**1***/**1a**.

Table 5. Energy Differences in kcal/mol (temperature, K) for **8/8*/8a**−**11/11*/11a**

	ΔH	ΔH_{expt}	ΔG (298)	ΔG_{expt}	E_A
8−**8a**	23.407		21.450		
8*−**8**	18.530	19.9[a]	19.459		20.5[a]
8*−**8a**	41.936		40.909		
9−**9a**	22.977		20.831		
9*−**9**	18.901		19.873		
9*−**9a**	41.878		40.703		
10−**10a**	22.444		21.305		
10*−**10**	19.901		20.121		19.4[b]
10*−**10a**	42.345		41.426		
11−**11a**	21.866		20.676		
11*−**11**	20.206		20.953		24.4[b]
11*−**11a**	42.073		41.629		

[a] Reference 13. [b] For 1,8-di-^{t}Bu derivative (Murakam, S.; Tsutsui, T.; Saito, S.; Yamato, T.; Tashiro, M. *Nippon Kagukukai Shi* **1988**, 221−229).

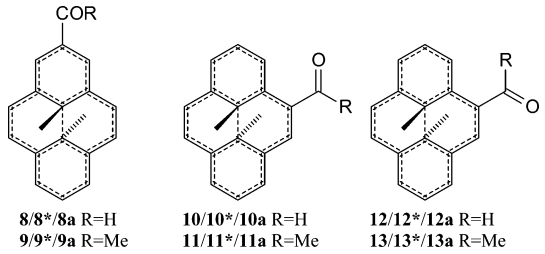

Substituting an acyl group at the 1- or 4-position of **1**/**1***/**1a** has little effect on their structures (Supporting Information Table S3). Of course, these substituents are conformationally mobile. Here we only consider the conformers corresponding with **10**/**10***/**10a** and **11**/**11***/**11a** and ignore the higher energy **12**/**12***/**12a** and **13**/**13***/**13a**.

Modifying the Activation Barrier

It is desirable to be able to design photoswitches with properties tailored to their applications. In this connection, we explored the possibility of affecting the barrier height to the CPD to DDP electrocyclization by specific substitution of the parent system. All of the TSs examined above were calculated to have significant biradical character ($\langle S^2 \rangle$ ranging from 0.76 for **2*** to 1.03 for **1***), and the unpaired electron density is the highest, or close to the highest, on C15/C16 for each molecule. We reasoned that substituting the parent compounds, especially at the 15- and 16-positions, with radical destabilizing groups should raise the energy of the TS and result in an increased activation barrier. Similarly, substitution with radical stabilizing groups was anticipated to lower this barrier. As already noted,

Table 6. Energies (kcal/mol), $\langle S^2 \rangle$, and Total Atomic Spin Densities for **8/8*/8a**−**11/11*/11a**

	total energy	total energy + ZPE	$\langle S^2 \rangle$	unpaired electrons C15 (C16)
8 (C_1)	−507527.0	−507343.6		
8* (C_1)	−507506.2	−507324.8	0.96	0.371 (0.370)
8a (C_1)	−507551.0	−507366.3		
9 (C_1)	−532202.1	−532001.1		
9* (C_1)	−532180.9	−531981.9	0.97	0.389 (0.392)
9a (C_1)	−532225.7	−532023.3		
10 (C_1)	−507526.5	−507342.7		
10* (C_1)	−507504.1	−507322.7	1.01	0.362 (0.391)
10a (C_1)	−507549.4	−507364.6		
11 (C_1)	−532199.7	−531998.4		
11* (C_1)	−532177.0	−531978.0	1.01	0.367 (0.395)
11a (C_1)	−532222.1	−532019.7		

and detailed in Table 5, substitution at the 1-position with radical stabilizing[20] acyl groups lowers the activation barrier for electrocyclization, while 4-acyl substituents are calculated to have little effect on the barrier. Supporting the notion that the greatest effect on the activation barrier will be produced by substitution at the centers of highest unpaired electron density, the unpaired electron density on the 1-position in **1*** is calculated to be the next highest to that at the 15/16-positions (and is large for all of the TSs).

We initially investigated trifluoromethyl substitution of **1**/**1***/**1a** with a view to *raising* the activation barrier. We chose the trifluoromethyl substituent as it is computationally economical and is known to destabilize radicals in the α-position.[20] Structurally, these trifluoromethyl derivatives, **14**/**14***/**14a**−**16**/**16***/**16a**, are similar to the other compounds studied (Supporting Information Table S4). The optimized structure for CPD **16** is of C_1 symmetry, while both DDP **16a** and TS **16*** are of C_{2h} symmetry. A nearly degenerate conformer of C_{2h} symmetry and almost identical geometry to **16** proved to be a transition structure (one imaginary frequency). Surprisingly, the calculated activation barriers for the 1- (**14**/**14***/**14a**), and 4- (**15**/**15***/**15a**) substituted derivatives are similar to those for the parent **1**/**1***/**1a**, and those for the 15,16-di- (**16**/**16***/**16a**) substituted derivative are *lower* than in **1**/**1***/**1a** (Table 7). Obviously, direct radical destabilization is not the principal factor in determining the height of the activation barrier.

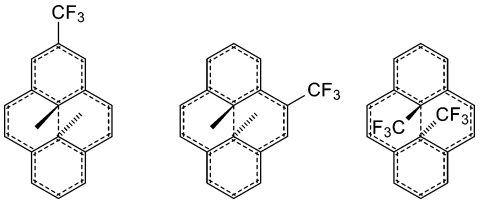

14/14*/14a **15/15*/15a** **16/16*/16a**

We next considered substitution with the radical stabilizing nitrile group, again chosen for its computational economy.[20] The calculated activation barrier for the 15,16-dinitrile **17** is significantly *larger* than that for **1**. In agreement with the results

(20) For the relative (de)stabilization of radicals see, for example: (a) Song, K.-S.; Liu, L.; Guo, Q.-X. *J. Org. Chem.* **2003**, *68*, 4604. (b) Henry, D. J.; Parkinson, C. J.; Mayer, P. M.; Radom, L. *J. Phys. Chem. A* **2001**, *105*, 6750. (c) Bordwell, F. G.; Zhang, X.-M.; Alnajjar, M. S. *J. Am Chem. Soc.* **1992**, *114*, 7623. (d) Pasto, D. J.; Krasnansky, R.; Zercher, C. *J. Org. Chem.* **1987**, *52*, 3062.

Table 7. Energy Differences in kcal/mol (temperature, K) for **14/14*/14a**−**16/16*/16a**

	ΔH	ΔG (298)
14−**14a**	22.570	20.893
14*−**14**	20.269	20.768
14*−**14a**	42.839	41.661
15−**15a**	22.179	20.292
15*−**15**	20.606	21.608
15*−**15a**	42.784	41.899
16−**16a**	24.641	22.167
16*−**16**	18.314	20.097
16*−**16a**	42.955	42.263

for the 1-acyl derivatives, **8** and **9**, the activation barriers for **18** and **19** are lower than for **1**. Nitrile substitution at the 1- and 8-positions has an additive effect, each nitrile group reducing the activation barrier of the parent **1** by approximately 1 kcal/mol. Substitution at the 2-, 7-, 9-, and 14-positions, the centers of lowest unpaired electron density in **1***, with the nitrile group has little effect on the calculated activation barrier, while with the trifluoromethyl group raises the barrier somewhat.

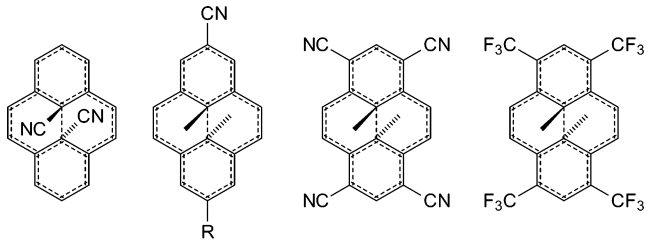

17/17*/17a **18/18*/18a** R=H **19/19*/19a** R=CN **20/20*/20a** **21/21*/21a**

Conclusions

Restricted density functional theory failed to model the TSs for the systems studied, forcing recourse to unrestricted density functional theory (UB3LYP). Each of these TSs was calculated to have considerable biradical character as indicated by their spin contaminated wave functions (nonzero $\langle S^2 \rangle$). Clearly, a spin contaminated solution cannot be "*the correct*" representation for a singlet species. However, several studies have shown that UB3LYP provides a reasonable modeling of biradicals and, for computationally large systems that are currently inaccessible for study at higher levels of theory, may provide the most reliable data. Indeed, recently, Davidson and Clark commented "until the reliability of a better model is established, broken spin DFT remains the most consistent choice for large molecules where complete active space with perturbation corrections is not feasible".[21] Similarly, Sakai demonstrated that for a series of electrocyclic reactions, including the forbidden conrotatory electrocyclization of 1,3,5-hexatriene, the UB3LYP and CASSCF geometries are in good agreement and the UB3LYP and MP2-CASSCF activation barriers agree qualitatively.[22]

Our results allow us to conclude that substitution at the positions of highest unpaired electron density in **1*** has the greatest effect. The radical stabilizing nitrile group at the 1,8-

(21) Davidson, E. R.; Clark, A. E. *Int. J. Quantum Chem.* **2005**, *103*, 1.
(22) Sakai, S. *Internet Electron. J. Mol. Des.* **2002**, *1*, 462.

Table 8. Energies (kcal/mol), $\langle S^2 \rangle$, and Total Atomic Spin Densities for **14/14*/14a**−**16/16*/16a**

	total energy	total energy + ZPE	$\langle S^2 \rangle$	unpaired electrons C15 (C16)
14 (C_1)	−647931.7	−647750.0		
14* (C_1)	−647908.6	−647728.1	1.01	0.393 (0.403)
14a (C_1)	−647885.9	−647707.6		
15 (C_1)	−647930.6	−647748.7		
15* (C_1)	−647908.0	−647727.2	1.02	0.406 (0.404)
15a (C_1)	−647884.8	−647706.3		
16 (C_1)	−810069.1	−809920.5		
16* (C_{2h})	−810044.2	−809896.3	0.99	0.411
16a (C_{2h})	−810023.3	−809877.8		

Table 9. Energy Differences in kcal/mol (temperature, K) for **17/17*/17a**−**21/21*/21a**

	ΔH	ΔG (298)
17−**17a**	11.139	11.139
17*−**17**	25.314	25.148
17*−**17a**	36.453	36.108
18−**18a**	23.146	21.206
18*−**18**	19.081	19.928
18*−**18a**	42.226	41.134
19−**19a**	22.722	20.922
19*−**19**	18.067	18.879
19*−**19a**	40.789	39.801
20−**20a**	23.234	21.696
20*−**20**	20.745	21.178
20*−**20a**	43.979	42.873
21−**21a**	19.568	20.018
21*−**21**	22.781	22.019
21*-21a	42.349	42.036

position(s) cause a decrease in the height of the barrier, while for 15,16-disubstitution, a large increase occurs. Radical destabilizing groups have essentially no effect at the 1-position and decrease the activation barrier when substituted at the 15,16-positions. Substitution at the 4-position with either radical stabilizing or destabilizing groups and at the 2,7,9,14-positions with radical stabilizing groups has little or no effect on the activation barrier. Radical destabilizing groups at the 2,7,9,14-positions raise this barrier slightly. Although a detailed evaluation of steric factors for each CPD, DDP, and TS and $\langle S^2 \rangle$ and unpaired electron densities for each TS failed to reveal any correlation between these parameters and the magnitude of the activation barriers, our results can be rationalized by considering the differences in energy between the substituted CPDs, TSs, and DDPs and the corresponding parent compounds **1**/**1***/**1a**. The change in energies upon substitution (ΔE) were obtained by subtracting the energies of **1** from the substituted CPDs, **1*** from the substituted TSs and **1a** from the substituted DDPs. These differences were scaled ($\Delta\Delta$), relative to each CPD, by subtracting ΔE_{CPD} from ΔE_{TS} and ΔE_{DDP} for each substituted derivative and are reported in Table 11 (positive values of $\Delta\Delta$ indicate relative destabilization, while negative values of $\Delta\Delta$ indicate relative stabilization). Analysis of the data in Table 11 reveals that the CPD **16** is "destabilized" relative to **16a** and **16***, while CPD **17** is "strongly stabilized" relative to **17a** and **17*** accounting for the lower (**16**) and higher (**17**) barriers. In CPD **16**, the electron-rich CF_3 groups are located directly over the opposing electron-rich phenyl rings (Figure 4), resulting in an unfavorable interaction. However, for CPD **17**, the nitrile groups are well aligned to conjugate with the phenyl rings to which they are attached (Figure 4). This conjugation stabilizes

Table 10. Energies (kcal/mol), $\langle S^2 \rangle$, and Total Atomic Spin Densities for **17/17*/17a**−**21/21*/21a**

	total energy	total energy + ZPE	$\langle S^2 \rangle$	unpaired electrons C15 (C16)
17 (C_{2h})	−502838.9	−502698.3		
17* (C_{2h})	−502810.8	−502672.9	1.15	0.428
17a (C_{2h})	−502850.1	−502709.2		
18 (C_s)	−494298.2	−494121.6		
18* (C_s)	−494276.8	−494102.2	0.98	0.390 (0.398)
18a (C_s)	−494321.9	−494144.0		
19 (C_{2h})	−552182.0	−552006.2		
19* (C_{2h})	−552161.7	−551987.9	0.96	0.371
19a (C_{2h})	−552205.2	−552028.3		
20 (C_{2h})	−667942.1	−667768.4		
20* (C_{2h})	−667918.7	−667747.5	1.08	0.435
20a (C_{2h})	−667966.0	−667791.0		
21 (C_{2h})	−1282386.1	−1282195.9		
21* (C_{2h})	−1282360.6	−502698.3	1.06	0.419
21a (C_{2h})	−1282406.0	−502672.9		

Table 11. Relative Stabilities ($\Delta\Delta = \Delta E - \Delta E_{CPD}$) in kcal/mol for **16/16*/16a**−**20/20*/20a**

	$\Delta\Delta E^a$	$\Delta\Delta$ZPE^b	$\Delta\Delta H^c$	$\Delta\Delta G^d$
$\Delta\Delta$**16a**	−1.151	−1.634	−1.457	−0.845
$\Delta\Delta$**16***	−2.036	−1.913	−1.987	−0.804
$\Delta\Delta$**17a**	12.436	11.535	12.045	10.362
$\Delta\Delta$**17***	5.171	4.832	5.0132	4.248
$\Delta\Delta$**18a**	−0.029	0.0659	0.038	0.116
$\Delta\Delta$**18***	−1.506	−1.1364	−1.220	−0.973
$\Delta\Delta$**19a**	0.493	0.454	0.462	0.400
$\Delta\Delta$**19***	−2.629	−2.146	−2.233	−2.022
$\Delta\Delta$**20a**	−0.179	−0.141	−0.050	−0.373
$\Delta\Delta$**20***	0.475	0.407	0.445	0.277

[a] Total energy. [b] Total Energy + ZPE. [c] Enthalpy. [d] Free energy.

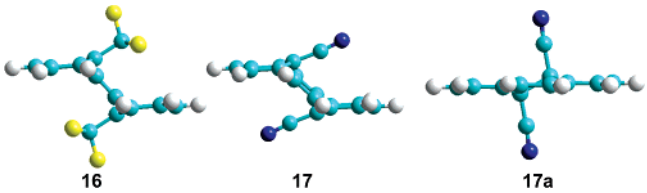

Figure 4. The optimized structures of **16**, **17**, and **17a**.

17 relative to the DDP **17a** in which the nitriles and phenyls are essentially orthogonal (Figure 4). The TSs **18*** and **19*** are "stabilized" relative to their corresponding CPDs and DDPs, no doubt due to the radical stabilization provided by the nitrile substituent(s). The results for **18**/**18***/**18a** ($\Delta\Delta$**18*** $\sim$ 1 kcal/mol) and **19**/**19***/**19a** ($\Delta\Delta$**19*** $\sim$ 2 kcal/mol) demonstrate that the effect of radical stabilization is small and easily overwhelmed by more powerful dipolar/steric (**16**) and conjugative (**17**) factors.

We found that of the systems studied, the 15,16-dinitrile **17**/**17***/**17a** has the highest calculated activation barrier of all ($\Delta H^{\ddagger}$ and $\Delta G^{\ddagger}$ (298) both about 25 kcal/mol). An activation barrier of this magnitude corresponds with a half-life of ~60 h at 46 °C, or several weeks at room temperature, which would certainly make it usable as a switch. The large $\langle S^2 \rangle$ (1.15) for **17*** prompts us to suggest that the barrier height in this system is probably underestimated by up to ~2 kcal/mol, which would result in an even greater lifetime for CPD **17**.

To some extent, these predictions have already been verified by the reported experimental activation energies for the acyl derivatives **8**−**11** (vide supra). The syntheses of appropriately

15,16-disubstituted compounds, especially the dinitrile **17**, represent worthy goals, which are certainly not trivial since many substituents are readily lost from the 15,16-positions, leading to pyrene derivatives.[23] We will report our efforts in this direction in the future.

(23) (a) Boekelheide, V.; Hylton, T. *J. Am. Chem. Soc.* **1970**, *92*, 3669. (b) Boekelheide, V.; Tsai, C. H. *J. Org. Chem.* **1973**, *38*, 3931. (c) Sawada, T.; Wakabayashi, M.; Takeo, H.; Miyazawa, A.; Tashiro, M.; Thiemann, T.; Mataka, S. *J. Chem. Soc., Perkin Trans. 1* **1999**, 403. (d) Lai, Y. H.; Zhou, Z. L. *J. Org. Chem.* **1997**, *62*, 925.

Acknowledgment. R.V.W. thanks Dr. Ken Ishida for his support of this research. R.H.M. thanks Science and Engineering Research Canada for financial support.

Supporting Information Available: Tables of geometric parameters, Cartesian coordinates for all optimized structures, and complete ref 10 (66 pages, print/PDF). This material is available free of charge via the Internet at http://pubs.acs.org.

JA054553R